

Rapid #: -11882767

CROSS REF ID: **293351**

LENDER: **UUM :: Marriott Library**

BORROWER: **ITD :: Eugene McDermott Library**

TYPE: Article CC:CCG

JOURNAL TITLE: Brain connectivity

USER JOURNAL TITLE: Brain Connectivity

ARTICLE TITLE: Evidence for Behaviorally Segregated, Spatiotemporally Overlapping Subnetworks in Phantom Sound Perception.

ARTICLE AUTHOR:

VOLUME: 7

ISSUE: 3

MONTH: Aug

YEAR: 2017

PAGES: 197-210

ISSN: 2158-0014

OCLC #:

Processed by RapidX: 5/5/2017 10:46:10 AM



This material may be protected by copyright law (Title 17 U.S. Code)

Evidence for Behaviorally Segregated, Spatiotemporally Overlapping Subnetworks in Phantom Sound Perception

Anusha Mohan,^{1,*} Nicole Moreno,^{1,*} Jae-Jin Song,² Dirk De Ridder,³ and Sven Vanneste¹

Abstract

One of the most intriguing questions in neuroscience is to understand the mechanism of information transfer between different brain areas. Recently, network theory has gained traction and is at the forefront of providing a possible explanation to not only the mechanism of information transfer but also in the identification of different neuropathologies. The perception of a phantom ringing in the ear called tinnitus, similar to other neuropathologies, has been shown to be accompanied by aberrant functional connectivity between different brain areas. Although, there have been independent studies showing that specific groups of areas encode individual symptoms of tinnitus, there has not been one study to show that tinnitus is the unified percept of distinguishable subnetworks encoding different behavioral aspects. This study combines resting-state functional connectivity obtained from the source-localized electroencephalography of 311 tinnitus patients and 264 controls, and a k-fold cross-validation machine learning algorithm to develop a predictive model that verifies the presence of behaviorally specific, spatiotemporally overlapping subnetworks in tinnitus. This reorganization is found to be exclusive to tinnitus, even when compared to physiologically similar disorders such as chronic pain, with each behavioral symptom having a unique oscillatory signature. This frequency-specific transmission of information, called multiplexing, enables different types of information to be carried between two brain regions through the same anatomical connection. In addition to understanding the efficient compensation mechanism of the brain in the presence of multisymptom disorders, the exclusivity of the prediction model presents an encouraging possibility for an objective neural marker for tinnitus.

Keywords: EEG; functional connectivity; multiplexing; source localization

Introduction

THE STUDY OF functional associations between interacting entities or network connectivity (Strogatz, 2001) has been rigorously investigated in various domains such as social (Strogatz, 2001), power supply (Albert et al., 2004), internet (Cohen et al., 2000, 2001), genetic (Barabasi et al., 2011; Goh et al., 2007), and brain networks (Bullmore and Sporns, 2009). Particular to brain networks, there has been an increased interest in understanding basic functions like development and learning (Papo et al., 2014), as well as to characterize changes in the structural and functional wiring patterns between different brain areas in the presence of a pathology (Fornito et al., 2015). The

network connectivity between different brain regions can be calculated as the coherence of the time series between the two areas (Pascual-Marqui, 2002; Pascual-Marqui et al., 2011) showing “communication through coherence” (Fries, 2005, 2015).

It has been suggested that brain networks assume a very cost-effective and efficient small-world topology, which facilitates segregation of brain areas into functionally separable modules and their integration over long distances by means of highly specialized regions called hubs (Bullmore and Sporns, 2009, 2012; Meunier et al., 2009). These functionally separable modules are found to spatially overlap given that different functional modules sometimes share common brain areas (Meunier et al., 2010; Yang and

¹Laboratory for Clinical and Integrative Neuroscience, School of Behavioral and Brain Sciences, The University of Texas at Dallas, Richardson, Texas.

²Department of Otorhinolaryngology-Head and Neck Surgery, Seoul National University Bundang Hospital, Bundang-gu, Seongnam, Korea.

³Section of Neurosurgery, Department of Surgical Sciences, Dunedin School of Medicine, University of Otago, Dunedin, New Zealand.

*These authors contributed equally to this work.

Leskovec, 2014). In addition, the same brain area may also be responsible for different tasks, facilitating processing of multimodal input at each location (Wu et al., 2011). Although aberration from small-world topology has been reported in the presence of a neuropathology (Agosta et al., 2013; Olde Dubbelink et al., 2014; Skidmore et al., 2011; Stam et al., 2009), the concept of functional modularity seems to be retained (Bassett et al., 2008), possibly driving an undesired efficiency in the disease network.

Tinnitus is the continuous phantom perception of a ringing or buzzing sound (Axelsson and Ringdahl, 1989; Jastreboff, 1990; Shargorodsky et al., 2010). The tinnitus network is characterized by an undesirable functional reorganization between auditory and nonauditory brain regions (Mohan et al., 2016a,b). In addition, the tinnitus network consists of a resilient core and a pliable periphery intertwined by overlapping subnetworks working in different oscillatory bands (Mohan et al., 2016c). In our previous work, we showed that although network reorganization in tinnitus is frequency band specific (Mohan et al., 2016a), these networks have overlapping brain areas across the different frequency bands (Mohan et al., 2016c). Furthermore, there also exists an evidence of networks of regions distinctly encoding the different behavioral aspects such as loudness (De Ridder et al., 2015; Vanneste and De Ridder, 2011), distress (Ueyama et al., 2013; Vanneste and De Ridder, 2011; Vanneste et al., 2010), and memory of the sensory deafferentation (De Ridder et al., 2013; Sedley et al., 2015). These subnetworks are identified in specific oscillatory bands, that is, the loudness network in the gamma frequency band (De Ridder et al., 2015), the distress network in the alpha and beta bands (Vanneste and De Ridder, 2011; Vanneste et al., 2010), and the memory of the deafferentation in the theta and gamma bands (De Ridder and Vanneste, 2014; De Ridder et al., 2013). These findings bring us to the theoretical model for tinnitus proposed by De Ridder and co-workers (2014b), which hypothesizes tinnitus as the unified percept of multiple, segregated behavioral symptoms encoded in multiple, spatially, and temporally overlapping subnetworks.

This evidence for temporally overlapping functional modules and neural signatures of behavioral correlates only alludes to the theoretical model for tinnitus. That is, there is no study that we are aware of, which combines the concept of overlapping networks with neural signature of behavioral correlates. To demonstrate this, the current study makes use of both resting-state functional connectivity and a machine learning algorithm to create a model that can discriminate the neuropathology, in this case tinnitus, from a control population. Machine learning algorithms have been used in combination with pathological changes in the cortical activity (Hu and Iannetti, 2016; Wager et al., 2013) and network connectivity (Chong et al., 2016; Eskildsen et al., 2015; Plitt et al., 2015), with the aim to extract distinct features from the disease network that can uniquely characterize the disorder. Although this technique helps in accurately discriminating a disorder from a control group, some researchers suggest that the model may fail when tested against disorders that show similar patterns of a neural activity or connectivity (Hu and Iannetti, 2016). For example, tinnitus has been suggested to resemble chronic pain owing to the similar etiology (i.e., deafferentation) (Folmer et al., 2001; Tonndorf, 1987).

In addition, it is suggested that tinnitus and chronic pain share, to a certain extent, similar brain networks that encode, for example, disorder-related distress (De Ridder et al., 2011a). However, the difference in the two disorders lies in the pathways that carry the two percepts. Pain has been identified by very specific nociceptive pathways that have not been identified in tinnitus yet (De Ridder et al., 2011a).

Hence, we hypothesize that the individual connections that help discriminate tinnitus from controls will be exclusive to tinnitus and will cluster into distinct groups of connections that correlate with a behavioral symptom. Furthermore, we hypothesize that these groups of connections will lie in specific oscillatory bands, yet have overlapping connections between brain areas across different groups. Thus, we expect that the behavioral correlate will have a neural oscillatory signature even when the connections between those brain areas possibly overlap across different subnetworks. Through this study, we thus try to provide empirical evidence for a disorder-specific reorganization of the brain as spatially and temporally overlapping subnetworks that behaviorally segregate into separable modules. We also try to establish that although this reorganization is specific to tinnitus, it is possible to understand the brain's coping mechanism to a disorder, from a network reorganization perspective. Furthermore, if the model is exclusive to tinnitus well above chance, then we also have a potential clinical diagnostic tool for tinnitus that can discriminate tinnitus from physiologically similar pathologies.

Materials and Methods

Subject groups

Tinnitus group. The tinnitus group consisted of 311 participants ($M=50.63$ years, standard deviation [SD]=13.67 years; 213 males and 98 females), the onset of whose percept occurred at least a year before data collection. Individuals having pulsatile tinnitus, Ménière's disease, otosclerosis, chronic headache, neurological disorders (such as brain tumors), and those being treated for mental disorders were excluded from the study. The qualitative aspects of tinnitus that were recorded included location (unilateral [$N=114$] or bilateral [$N=197$]) and type (pure tone [$N=118$] or noise like [$N=193$]). Pure-tone audiometric thresholds were collected at 0.125, 0.25, 0.5, 1, 2, 3, 4, 6, and 8 kHz as recommended by the British Society of Audiology. Further diagnostic measurements included identifying the pitch and loudness of the tinnitus on the side with the strongest sense of the tinnitus percept. This was done by presenting a 1 kHz pure tone, 10 dB above the patient's hearing threshold at that frequency, in the ear contralateral to that of the tinnitus percept. The pitch of tinnitus was determined by adjusting the frequency of the pure tone until the patient matched it to the pitch of the percept. The intensity of the pure tone was changed to determine the loudness of the percept. Tinnitus loudness level (dB SL) ($M=7.85$ dB SL, $SD=8.78$) was then calculated by subtracting the absolute loudness level from the audiometric threshold at the tinnitus frequency ($M=5143$ Hz, $SD=3183$) (Meeus et al., 2010, 2011). A visual analogue scale for loudness (VAS) ("How loud is your tinnitus?": 0=no tinnitus and 10=as loud as imaginable) was assessed. The mean VAS for loudness was 5.31 ($SD=2.56$). Also, the Tinnitus Questionnaire (TQ) (Meeus

et al., 2007) was assessed that measures a broad spectrum of tinnitus-related psychological complaints. The global TQ score can be computed to measure the general level of psychological and psychosomatic distress. The mean score on the TQ was 36.45 (SD=17.32). The depression and anxiety were evaluated using the Hospital Anxiety and Depression Scale. The mean score on the depression scale was 6.50 (SD=4.06) and the mean score on the anxiety scale was 6.52 (SD=3.48).

Control group. The healthy control group consisted of 264 participants ($M=49.78$ years; $SD=14.74$; 154 males and 110 females). Individuals with psychiatric and neurological illness, a history of psychiatric disorders and drug/alcohol abuse, records of head injury that resulted in a loss of consciousness, seizures, headaches, and physical disability were excluded from the study. No audiometric testing was done on the individuals in the control group.

Neuropathic pain group. The group consisting of patients suffering from neuropathic pain comprised 78 participants ($M=52.41$ years; $SD=11.52$; 45 males and 33 females). The term “Neuropathic pain,” related to deafferentation, that is, peripheral nerve, root or central tract lesions, as used in this study, is an umbrella term that encompasses individuals suffering from chronic pain. These patients suffered from these pain complaints for more than 1 year. A numeric rating scale for pain (“How much pain do you have?”: 0=no pain and 10=as painful as imaginable) assessed the perceived general pain. General pain was defined as a global pain score experienced during the past week. The mean pain score on the numeric rating scale was 8.15 (SD=2.98). The Pain Vigilance and Awareness Questionnaire (PVAQ) was also assessed. The PVAQ measures the preoccupation with or attention to pain and pain changes, and is associated with pain-related fear and perceived pain severity (Roelofs et al., 2003). It consists of two separable factors that measure (1) attention to pain and (2) attention to changes in pain (Roelofs et al., 2003). For the PVAQ, the baseline score for attention to pain was 13.60 (SD=4.21) and for attention to changes in pain was 17.57 (SD=3.98).

Tinnitus group for validation of exclusivity. An additional group of 53 tinnitus patients ($M=48.91$ years, $SD=13.02$ years; 26 males and 27 females) was collected to test the tinnitus models. Fifteen patients had unilateral tinnitus and 34 had bilateral tinnitus. Twenty-one patients had pure-tone tinnitus, while 32 reported to have noise-like tinnitus. The average tinnitus loudness level (dB SL) was 6.24 dB SL (SD=6.02) and the tinnitus frequency was 4845 Hz (SD=2071). The mean VAS for loudness was 6.04 (SD=3.09). The mean score on the TQ was 40.91 (SD=20.75).

Data collection and preprocessing

Data collection. The data were collected under the approval of IRB UZA OGA85. All patients gave an informed consent (as in accordance with the declaration of Helsinki and approved by the local ethics committee at Antwerp University Hospital). Continuous resting-state electroen-

cephalography (EEG) was recorded for 5 min from participants in all three groups (sampling rate=500 Hz, band passed=0.15–200 Hz). Subjects were seated upright on a comfortable chair in a fully lit room and were instructed to keep their eyes closed. The EEGs were sampled using Mistar-201 amplifiers (NovaTech; www.novatecheeg.com/) with 19 electrodes arranged in the International 10–20 standard placement (Fp1, Fp2, F7, F3, Fz, F4, F8, T7, C3, Cz, C4, T8, P7, P3, Pz, P4, P8, O1, and O2). The electrodes were referenced to digitally linked ears and the impedances were kept under 5 k Ω . Off-line analyses included resampling the data at 128 Hz and filtering using a 2–44 Hz band-pass filter. These data were then exported into Eureka! software (Congedo, 2002) where it was plotted and manually inspected for episodic artifacts (including eye blinks, eye movement, teeth clenching, body movement, and electrocardiography [ECG]), which were subsequently removed from the EEG. Average Fourier cross-spectral matrices were then computed for the eight frequency bands previously researched in tinnitus: Delta (2–3.5 Hz), Theta (4–7.5 Hz), Alpha1 (8–10 Hz), Alpha2 (10–12 Hz), Beta1 (13–18 Hz), Beta2 (18.5–21 Hz), Beta3 (21.5–20 Hz), and Gamma (30.5–44 Hz).

Data preprocessing. Source reconstruction was generated by estimating the intracerebral electrical sources through standardized low-resolution brain electromagnetic tomography [sLORETA; Pascual-Marqui (2002)]. As a standard practice before the execution of the sLORETA algorithm, a common average reference transformation was performed on the data (Pascual-Marqui, 2002). sLORETA differs from other source localization algorithms since it does not assume a predefined number of active sources, while computing neuronal activity in current density (A/m²). The solution space and the associated lead field matrix used in the study were those that were implemented using the LORETA-Key software (available at www.uzh.ch/keyinst/loreta.htm). The neocortical (including the hippocampal and anterior cingulate cortex) MNI-152 volume was divided and labeled according to the sLORETA-Key anatomical template based on probabilities returned by the Deamon Atlas (Lancaster et al., 2000) on a total of 6239 voxels (5 mm³ each).

Lagged phase coherence. The lagged-phase coherence has been interpreted as contributing to source activity by cross talk between brain regions (Congedo et al., 2010). In another way, if the oscillations of two sources are coherent with phase lag, this cross talk could be interpreted as axonal transmission of shared information. This signal can be decomposed by the discrete Fourier transformation into a finite series of sine and cosine waves (carrier out-of-phase and in-phase waves, which compose the real and imaginary portion of the Fourier decomposition) at the Fourier frequencies (Bloomfield, 2000). Lag of cosine waves is inversely proportional (with respect to sine counterparts) to their frequency. Pascual-Marqui defined lagged-phase coherence and also described the significance thresholds for given set of lagged-phase coherence values according to asymptotic results (Pascual-Marqui et al., 2011). In this study, the amount of lagged-phase coherence between interacting regions represents the connectivity strength between pairwise combinations of 84 Brodmann areas. The 84 Brodmann areas used in this study are defined in Table 1.

TABLE 1. BRODMANN AREAS AND ABBREVIATIONS USED IN THE STUDY

<i>Brodman areas</i>	<i>Abbreviation</i>	<i>Name of the Brodman area</i>
BA01	S1	Primary Somatosensory Cortex
BA02	S2	Secondary Somatosensory Cortex
BA03	S3	Tertiary Somatosensory Cortex
BA04	M1	Primary Motor Cortex
BA05	SPS	Superior Parietal Sulcus
BA06	SMA	Supplementary Motor Area
BA07	SPG	Superior Parietal Gyrus
BA08	Pre-SMA	Pre-supplementary Motor Area
BA09	DLPFC	Dorsolateral Pre-frontal Cortex
BA10	FPC	Fronto-Parietal Cortex
BA11	OFC	Orbital Frontal Cortex
BA13	Insula	Insula
BA17	V1	Primary Visual Cortex
BA18	V2	Secondary Visual Cortex
BA19	Cuneus	Cuneus
BA20	ITG	Inferior Temporal Gyrus
BA21	MTG	Medial Temporal Gyrus
BA22	STG	Superior Temporal Gyrus
BA23	PCC1	Posterior Cingulate Cortex1
BA24	dACC	Dorsal Anterior Cingulate Cortex
BA25	sgACC	Subgenual Anterior Cingulate Cortex
BA27	PHC1	Parahippocampal Gyrus1
BA28	HIP1	Hippocampal Area1
BA29	RSC1	Retrosplenial Cortex1
BA30	RSC2	Retrosplenial Cortex2
BA31	PCC2	Posterior Cingulate Cortex2
BA32	prACC	Pregenuar Anterior Cingulate Cortex
BA33	rACC	Rostral Anterior Cingulate Cortex
BA34	HIP	Hippocampus
BA35	HIP2	Hippocampal Area2
BA36	PHC2	Parahippocampal Gyrus2
BA37	OTC	Occipital-Temporal Cortex
BA38	TP	Temporal Pole
BA39	AG	Angular Gyrus
BA40	IPS	Intraparietal Sulcus
BA41	A1	Primary Auditory Cortex
BA42	A2	Secondary Auditory Cortex
BA43	PCG	Post-central Gyrus
BA44	OPCG	Opercular Part of Inferior Frontal Gyrus
BA45	IFG	Inferior Frontal Gyrus
BA46	MPFC	Medial Prefrontal Cortex
BA47	VLPFC	Ventrolateral Prefrontal Cortex

Model generation

Tenfold cross validation. The pairwise connectivity strengths (weights) in the different frequency bands were further organized into a file that could be read by the data-mining software Weka (University of Waikato Machine Learning Group, available at www.cs.waikato.ac.nz/ml/weka). Thus, the file consisted of the full dataset, which comprised the pairwise connectivity weights of 311 tinnitus and 264 control participants between 84 Brodmann areas in the 8 frequency bands. Using a simple logistics filter, a 2–10-

fold cross-validation was performed on the full dataset to generate a learning curve through the different models generated to classify the instances with tinnitus. From these different models, the most important contributing connections, which contrast the tinnitus from control networks, were extracted. Cross-validation is a technique in which the data set is divided into k equal portions called folds. The first fold is used to generate a predictive model of the dataset. The data in the remaining $k - 1$ -folds are then tested against the model yielding measurements of model accuracy. A second model is then generated off the second fold and the remaining $k - 1$ -folds (which include the fold that created the first model) are tested against this new model again. Subsequently, after all the folds have been used to create and test a model, the average of the values of model accuracy over the k -fold cross-validation is presented as the overall accuracy of the model. For example, in a 10-fold cross-validation technique, k_1 would consist of 10% of the entire dataset to generate the first model, and each of the nine remaining folds (k_2-k_{10}) is used as test sets. At the end of a 10-fold validation, a total of 90 values of model accuracy would be averaged together to obtain the overall accuracy of the model.

The measurements of model accuracy calculated by the k -fold cross-validation technique include the number of correctly classified cases, number of incorrectly classified cases, true-positive ratio, root mean squared error (RMSE), mean average error (MAE), and κ -statistic. The true-positive ratio was calculated as the ratio of the total number of correctly classified positive instances (in this case, positive refers to tinnitus patients) over the total number of positive instances in the testing sample. RMSE is a measure of how well the model is learned by the machine and was calculated by taking the square root of the average of the residuals (errors not explained by the regression equation) over the total sample size. The mean average error (MAE) is simply the average of residuals over the total sample size. The κ -statistic compares the model's observed accuracy with its expected (chance) accuracy by taking the difference in observed and expected accuracy over one minus the expected accuracy (1—expected accuracy).

Randomization of data. To determine significance of the model accuracy for the tinnitus/control model, measurements of model accuracy were averaged over 20 iterations of randomized assignment of patient data as either tinnitus or control. The randomized dataset was then used to generate a prediction model and model accuracy values, which were averaged across the 20 trials. The number of records assigned to tinnitus ($n = 311$) and controls ($n = 264$) was kept constant across all iterations to minimize variance compared to the original model.

Validation of exclusivity. Using the tinnitus model generated by the 10-fold cross-validation technique in Weka, an additional test set consisting of network connectivity strengths of the functional networks derived from 78 neuropathic pain patients and 53 tinnitus patients was validated. Similar to the cross-validation technique used for creating the tinnitus model, this dataset was divided into 10-folds where each fold of data was tested against the previously generated tinnitus model. The resulting measurement of model

accuracy was calculated on the tinnitus/pain model as mentioned above. To test the significance of the tinnitus/pain model, the measurements of model accuracy were averaged over 20 iterations of randomly assigning patients to either the tinnitus group or the neuropathic pain group. The number of patients assigned to the tinnitus group $n=53$ and the pain group ($n=78$) was maintained during the randomization process to minimize variance with respect to the original model.

Statistical test

On obtaining the averaged measurements of model accuracy from the tinnitus/control, tinnitus/pain, and the randomizations, a chi-square test was performed to determine the significance of the tinnitus/control and the tinnitus/pain models against the random models. The χ^2 values were calculated using the observed values of number of correctly and incorrectly classified cases from the 10-fold cross-validation results of the tinnitus/control and tinnitus/pain models and the expected values of number of correctly and incorrectly classified cases from the corresponding random models.

A four-factor principal component analysis (PCA) was conducted between the tinnitus contributing connections and behavioral measures collected using IBM SPSS 22 software. This factor analysis was then overlaid on the original tinnitus model to determine which clusters of connections demonstrate significant correlation with specific behavioral measures. In addition to the original factor analysis, partial correlation analysis was performed on the significant behavioral measures with each factor, while controlling for behavioral measures that showed a significant correlation with the measure in question.

Results

Tinnitus model

The tinnitus model generation using the cross-validation technique resulted in identifying a set of 65 connections that uniquely differentiate the functional networks of the tinnitus and control groups. These contributing connections span across the eight frequency bands and two hemispheres. All models generated using 2–10-folds comprised the same 65 contributing connections and resulted in the same contributing values (β values) and values of model accuracy (Fig. 1). True-positive discrimination accuracy ranged from 0.82 (2-folds) to 0.88 (6-, 9-, and 10-folds). RMSE was confined to a range between 0.31 (6-, 7-, 9-, and 10-folds) and 0.35 (2-folds).

Due to the increased statistical significance of the 10-fold cross-validation over a 2-fold cross-validation, as reported in previous research (Lemm et al., 2011), the remainder of this study will report the findings from the tinnitus model generated using the 10-fold cross-validation. The generated tinnitus model was fairly accurate at distinguishing between tinnitus and control patients with the percentage of correctly classified cases = 87.70%, percentage of incorrectly classified cases = 12.35%, κ -statistic = 0.75, MAE = 0.20, and RMSE = 0.31 (Fig. 2).

Randomization results

Randomization of the tinnitus/control model yielded a model where the percentage of correctly classified cases = 52.41%, percentage of incorrectly classified cases = 47.60%, κ -statistic = -0.002, MAE = 0.50, and RMSE = 0.51. Randomization of the tinnitus/control data demonstrated that the tinnitus prediction model was significant when compared to the averaged randomized prediction model ($\chi^2=286.35$, $p<0.001$) (Fig. 2).

Connections of importance

The 65 connections that discriminate the tinnitus from the control are named the connections of importance. These connections span into two large clusters with more than five connections, five smaller clusters with two to five connections, and six single-connection clusters that were not grouped together by brain hemisphere or oscillatory frequency bands (Fig. 3).

Behavioral correlates

PCA of the contribution of each of the connections of importance (β values) from the tinnitus model generated and the behavioral data collected from tinnitus participants demonstrated a high correlation between factors and frequency bands for contributing connections (Table 2). Factor 1 comprised every contributing connection in theta, beta1, beta2, beta3, and gamma frequency bands along with several alpha1 contributing connections that overlap with Factor 4 and alpha2 contributing connections that overlap with Factor 2. The rest of the contributing connections in Factor 2 are present in the alpha2 band, while the remaining contributing connections in Factor 4 are present in the alpha1 band. All the contributing connections in Factor 3 belong to the delta band. A more detailed description of the connections in

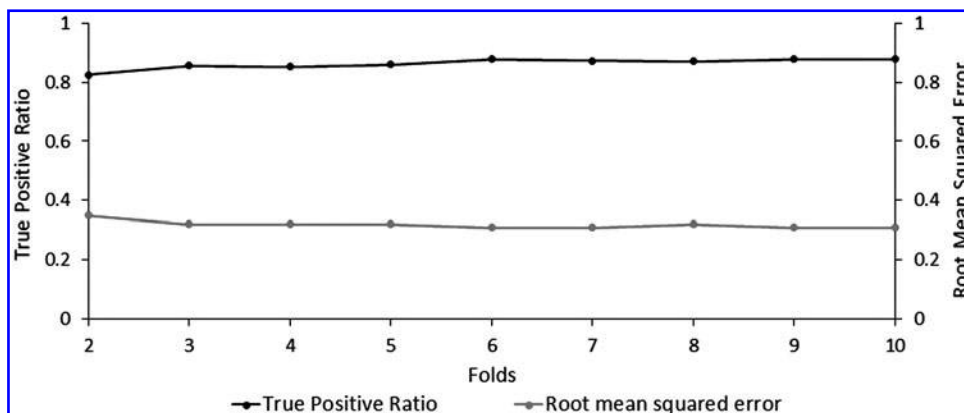


FIG. 1. Accuracy and error in tinnitus discrimination across multiple cross-validation trials. The ratio of true positive tinnitus predictions (black) and their corresponding RMSE (gray) across 2–10 cross-validation folds. RMSE, root mean square error.

FIG. 2. Evaluation of the accuracy and exclusivity of the tinnitus prediction model. (A) Demonstrates the percent correctly (black) and incorrectly (gray) classified between the (a) original tinnitus/control dataset, (b) randomized tinnitus/control dataset, (c) tinnitus/pain dataset, and (d) randomized tinnitus/pain dataset evaluated using the 10-folds cross-validation technique. (B) Compares the measurements of model accuracy such as the κ -statistic (black), MAE (dark gray), and RMSE (light gray) in the (a) original tinnitus/control model, (b) randomized tinnitus/control model, (c) tinnitus/pain dataset tested against the original model, and (d) randomization of the tinnitus/pain dataset. MAE, mean average error.

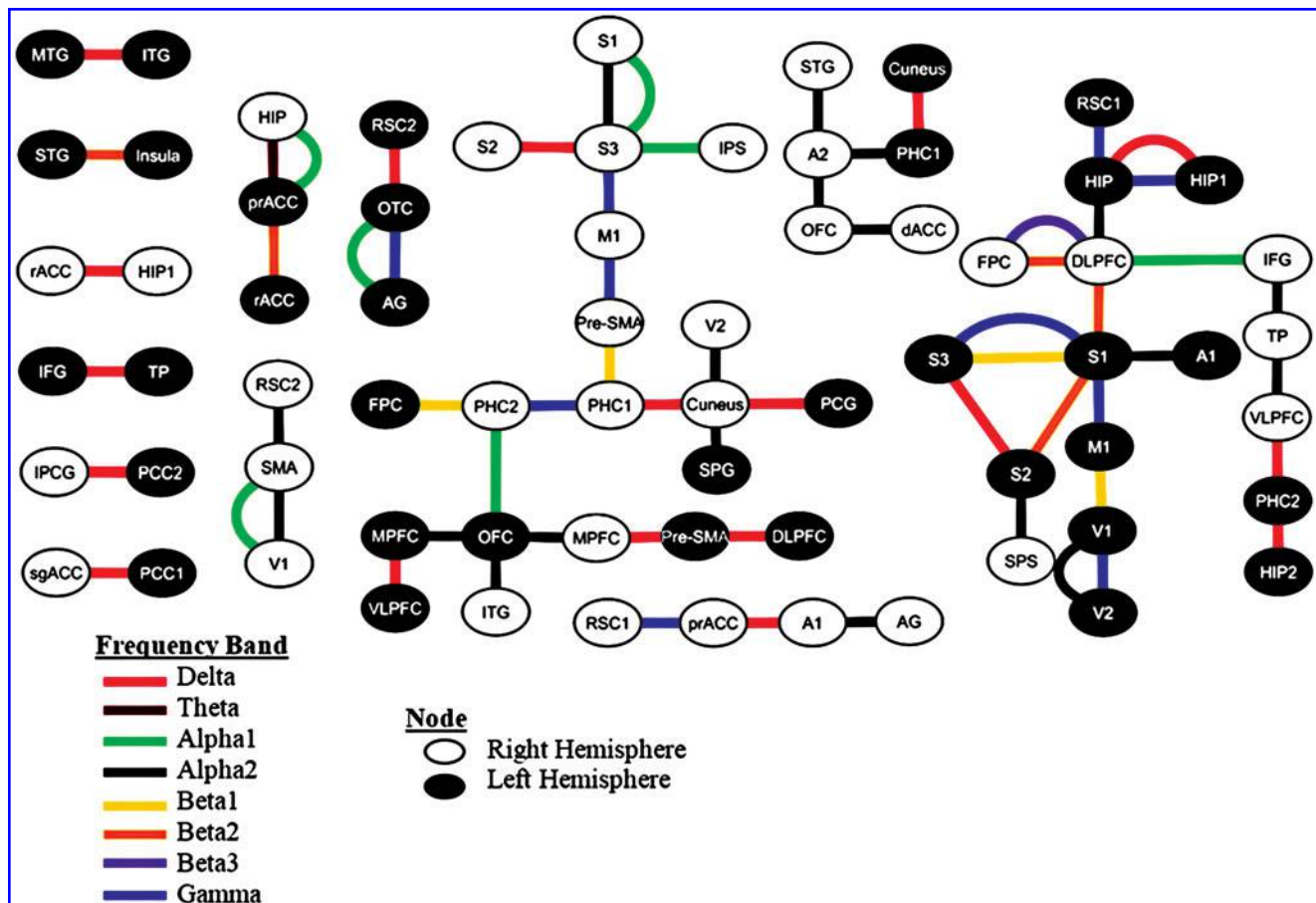
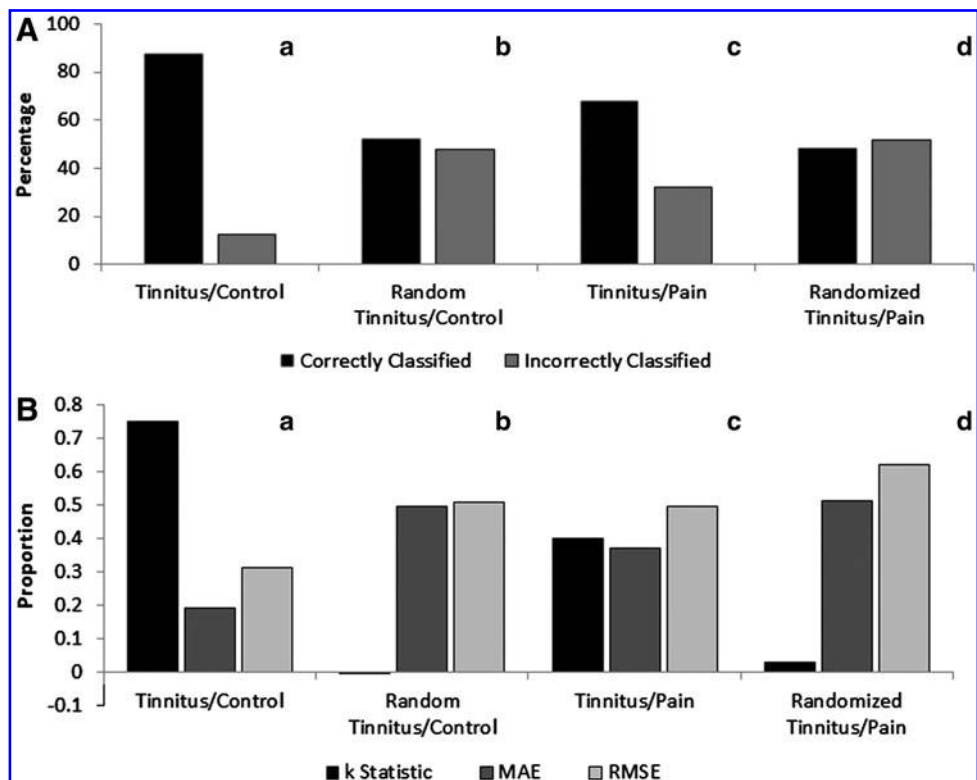


FIG. 3. Connections of importance as generated by the original tinnitus model using the 10-fold cross-validation. Brodmann brain regions are connected over frequency bands *delta* (red line), *theta* (brown line), *alpha1* (green line), *alpha2* (black line), *beta1* (yellow line), *beta2* (orange line), *beta3* (purple line), and *gamma* (blue line). Implicated Brodmann areas were also differentiated based on location on either the right (white circle) or left (black circle) hemispheres. Color images available online at www.liebertpub.com/brain

TABLE 2. CONTRIBUTING CONNECTIONS FROM TINNITUS PREDICTION MODEL

Connection	Frequency band	b-value	Component			
			Factor 1	Factor 2	Factor 3	Factor 4
Right S3–Right M1	Gamma	2.05	0.90	0.15	0.14	0.25
Left V1–Left V2	Gamma	–1.72	0.87	0.15	0.16	0.16
Left OTC–Left AG	Gamma	–0.38	0.87	0.14	0.16	0.22
Left S1–Left S3	Gamma	0.75	0.85	0.09	0.04	0.30
Left S1–Left M1	Gamma	1.20	0.84	0.08	0.03	0.30
Right DLPFC–Right FPC	Beta2	–0.29	0.84	0.14	0.19	0.15
Right PHC1–Right PHC2	Gamma	–0.7	0.82	0.16	0.18	0.11
Left HIP1–Left HIP	Gamma	–0.41	0.81	0.13	0.20	0.07
Left S1–Right DLPFC	Beta2	2.4	0.81	0.24	0.37	0.11
Left RSC1–Left HIP	Gamma	–1.53	0.80	0.09	0.12	–0.03
Right Pre-SMA–Right PHC1	Beta1	1.68	0.79	0.29	0.30	0.15
Right DLPFC–Right FPC	Beta3	–0.54	0.78	0.05	0.10	0.26
Left S1–Left S3	Beta1	0.34	0.76	0.25	0.29	0.11
Right M1–Right Pre-SMA	Gamma	–0.91	0.75	0.07	–0.03	0.23
Left FPC–Right PHC2	Beta1	1.83	0.75	0.14	0.17	0.12
Left Insula–Left STG	Beta2	–0.84	0.73	0.23	0.35	0.13
Left prACC–Left rACC	Beta2	–0.73	0.73	0.16	0.25	0.14
Right DLPFC–Right IFG	Alpha1	0.23	0.66	0.13	0.09	0.54
Left M1–Left V1	Beta1	–0.93	0.66	0.16	0.37	0.11
Left S1–Left S2	Beta2	0.32	0.63	0.23	0.33	0.19
Left prACC–Right HIP	Theta	2.7	0.63	0.12	0.29	0.20
Right RSC1–Right prACC	Gamma	1.84	0.59	0.04	0.03	–0.13
Left OFC–Left MPFC	Alpha2	0.28	0.59	0.57	0.23	0.04
Right SMA–Right V1	Alpha2	–0.33	–0.01	0.90	0.05	0.08
Right SMA–Right RSC2	Alpha2	–0.52	–0.05	0.87	–0.02	0.12
Right AG–Right A1	Alpha2	–0.19	–0.04	0.84	–0.02	0.13
Left SPG–Right Cuneus	Alpha2	–0.32	0.17	0.83	0.06	0.08
Left PHC1–Right A2	Alpha2	0.45	0.26	0.83	0.17	0.11
Left S1–Left A1	Alpha2	–0.21	0.10	0.82	0.02	0.12
Right V2–Right Cuneus	Alpha2	0.1	0.00	0.80	0.04	0.01
Left V1–Left V2	Alpha2	0.16	–0.01	0.80	0.05	0.01
Left S2–Right SPS	Alpha2	–0.41	0.36	0.76	0.12	0.15
Right OFC–Right A2	Alpha2	0.46	0.27	0.76	0.19	0.05
Right STG–Right A2	Alpha2	0.32	0.37	0.76	0.06	0.15
Left OFC–Right ITG	Alpha2	0.71	0.34	0.73	0.17	0.01
Right S1–Right S3	Alpha2	0.1	0.05	0.72	–0.05	0.22
Right OFC–Right dACC	Alpha2	–0.46	0.41	0.69	0.15	0.11
Right TP–Right IFG	Alpha2	–0.27	0.49	0.66	0.19	0.17
Right TP–Right VLPFC	Alpha2	–0.17	0.51	0.63	0.20	0.15
Left OFC–Right MPFC	Alpha2	0.64	0.57	0.61	0.23	0.07
Left HIP–Right DLPFC	Alpha2	0.76	0.59	0.61	0.28	0.10
Left PHC2–Right VLPFC	Delta	1.57	0.18	0.07	0.86	–0.03
Left PCC2–Right IPCG	Delta	–1.51	0.06	0.07	0.84	0.09
Left HIP2–Left PHC2	Delta	–0.8	0.28	0.13	0.83	–0.03
Right HIP1–Right rACC	Delta	1.51	0.07	0.03	0.81	0.00
Right prACC–Right A1	Delta	1.83	0.14	0.010	0.80	–0.02
Left PCC1–Right sgACC	Delta	4.1	0.32	0.15	0.79	–0.02
Left Cuneus–Left PHC1	Delta	1.5	0.18	0.03	0.79	0.04
Left Pre-SMA–Right MPFC	Delta	–1.46	0.01	0.01	0.78	0.05
Left ITG–Left MTG	Delta	0.75	0.02	0.09	0.77	0.02
Left TP–Left IFG	Delta	–1.32	0.33	0.13	0.76	–0.01
Left HIP1–Left HIP	Delta	–1.28	0.25	0.13	0.74	–0.05
Left RSC2–Left OTC	Delta	1.12	0.15	–0.01	0.72	0.01
Left PCG–Right Cuneus	Delta	–1.95	0.22	0.09	0.71	–0.01
Right S2–Right S3	Delta	–0.33	0.13	0.04	0.69	0.01
Left MPFC–Left VLPFC	Delta	0.51	0.03	0.10	0.67	–0.02
Left S2–Left S3	Delta	–0.23	0.25	0.03	0.63	0.01
Right Cuneus–Right PHC1	Delta	1.92	0.16	–0.03	0.62	0.08
Left Pre-SMA–Left DLPFC	Delta	–0.21	0.05	0.09	0.58	0.03
Right SMA–Right V1	Alpha1	–0.38	0.15	0.18	–0.03	0.86
Left OFC–Right PHC2	Alpha1	0.67	0.43	0.11	–0.02	0.77
Right S1–Right S3	Alpha1	0.09	0.32	0.21	0.01	0.76
Right S3–Right IPS	Alpha1	–0.12	0.24	0.19	–0.02	0.76
Left OTC–Left AG	Alpha1	–0.28	0.22	0.21	0.02	0.71
Left prACC–Right HIP	Alpha1	0.65	0.33	0.16	0.05	0.68

Bold values denote significant contribution of the connections in that particular factor.

importance and their contribution to each factor is given in Table 2 and illustrated in Figure 4.

Factor 1 was significantly correlated with depression ($r=0.10$, $p=0.048$) (Fig. 5A). Factor 2 showed significant correlation with age ($r=0.23$, $p<0.001$), duration of percept ($r=-0.14$, $p=0.008$), loudness of percept ($r=-0.12$, $p=0.017$), and mean hearing loss (MHL) ($r=-0.25$, $p=0.002$) (Fig. 5B). A significant correlation was observed between Factor 3 and distress, that is, TQ ($r=-0.15$, $p=0.007$) (Fig. 5C). Factor 4 showed a significant correlation with age ($r=0.16$, $p=0.003$) and MHL ($r=0.22$, $p=0.006$) (Fig. 5D). From the results of the partial correlation detailed in Table 3, we observe that Factor 1 was significantly correlated with the TQ score after controlling for tinnitus-related anxiety ($r=0.10$, $p=0.047$) and significantly correlated with tinnitus-related depression after controlling for the loudness of the percept ($r=0.10$, $p=0.048$); Factor 2 was significantly negatively correlated with age after controlling for tinnitus-related anxiety ($r=-0.23$, $p<0.001$), duration ($r=-0.20$, $p=0.001$), loudness of the percept ($r=-0.19$, $p<0.001$), and MHL ($r=-0.15$, $p=0.049$); was significantly negatively correlated with tinnitus-related depression after controlling for TQ score ($r=-0.11$, $p=0.043$); was significantly negatively correlated with the loudness of the percept after controlling for TQ score ($r=-0.10$, $p=0.043$); was significantly negatively correlated with MHL after controlling for TQ score ($r=-0.27$, $p=0.001$), tinnitus-related depression ($r=-0.22$, $p=0.008$), duration ($r=-0.20$, $p=$

0.02), and loudness ($r=-0.23$, $p=0.005$) of the percept. Factor 3 was significantly correlated with age after controlling for MHL ($r=0.21$, $p=0.008$); was significantly negatively correlated with TQ score after controlling for tinnitus-related anxiety ($r=-0.14$, $p=0.011$) and depression ($r=-0.12$, $p=0.028$), duration ($r=-0.15$, $p=0.01$), and loudness of the percept ($r=-0.16$, $p=0.004$). Factor 4 was significantly correlated with age after controlling for anxiety ($r=0.17$, $p=0.004$), duration ($r=0.17$, $p=0.003$), and loudness of the percept ($r=0.18$, $p=0.001$); was significantly negatively correlated with the loudness of the percept after controlling for MHL ($r=-0.18$, $p=0.021$); was significantly correlated with MHL after controlling for age ($r=0.20$, $p=0.013$), TQ score ($r=0.23$, $p=0.005$), tinnitus-related depression ($r=0.23$, $p=0.007$), duration ($r=0.19$, $p=0.024$), and loudness of the percept ($r=0.27$, $p=0.001$).

Exclusivity of the model

The tinnitus/control model when tested against the tinnitus/pain dataset had a better-than-chance success rate at distinguishing between tinnitus from neuropathic pain patients. The model yielded percentage of correctly classified cases = 66.40%, percentage of incorrectly classified cases = 31.88%, κ -statistic = 0.40, MAE = 0.38, and RMSE = 0.50. Randomization of the tinnitus/pain dataset yielded a model with percentage of correctly classified cases = 48.48%, percentage of incorrectly classified cases = 51.52%, κ -statistic = 0.40,

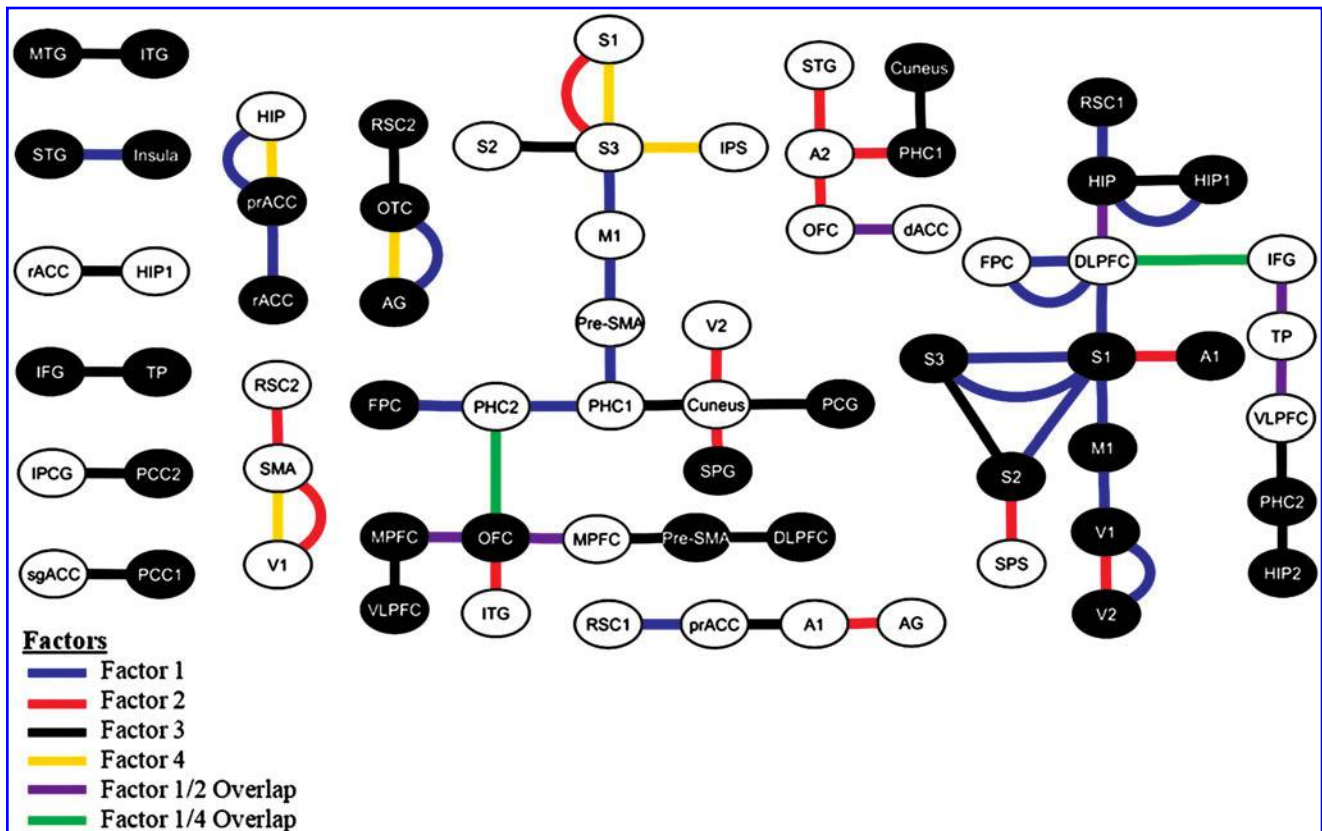


FIG. 4. Classification of the connections of importance into factors as determined by PCA. Connections were attributed to Factor 1 (blue), Factor 2 (red), Factor 3 (black), and Factor 4 (yellow). Several connections contributed to more than one factor; these fell into the Factor 1/Factor 2 overlapping connections (purple) and the Factor 1/Factor 4 overlapping connections (green). PCA, principal component analysis. Color images available online at www.liebertpub.com/brain

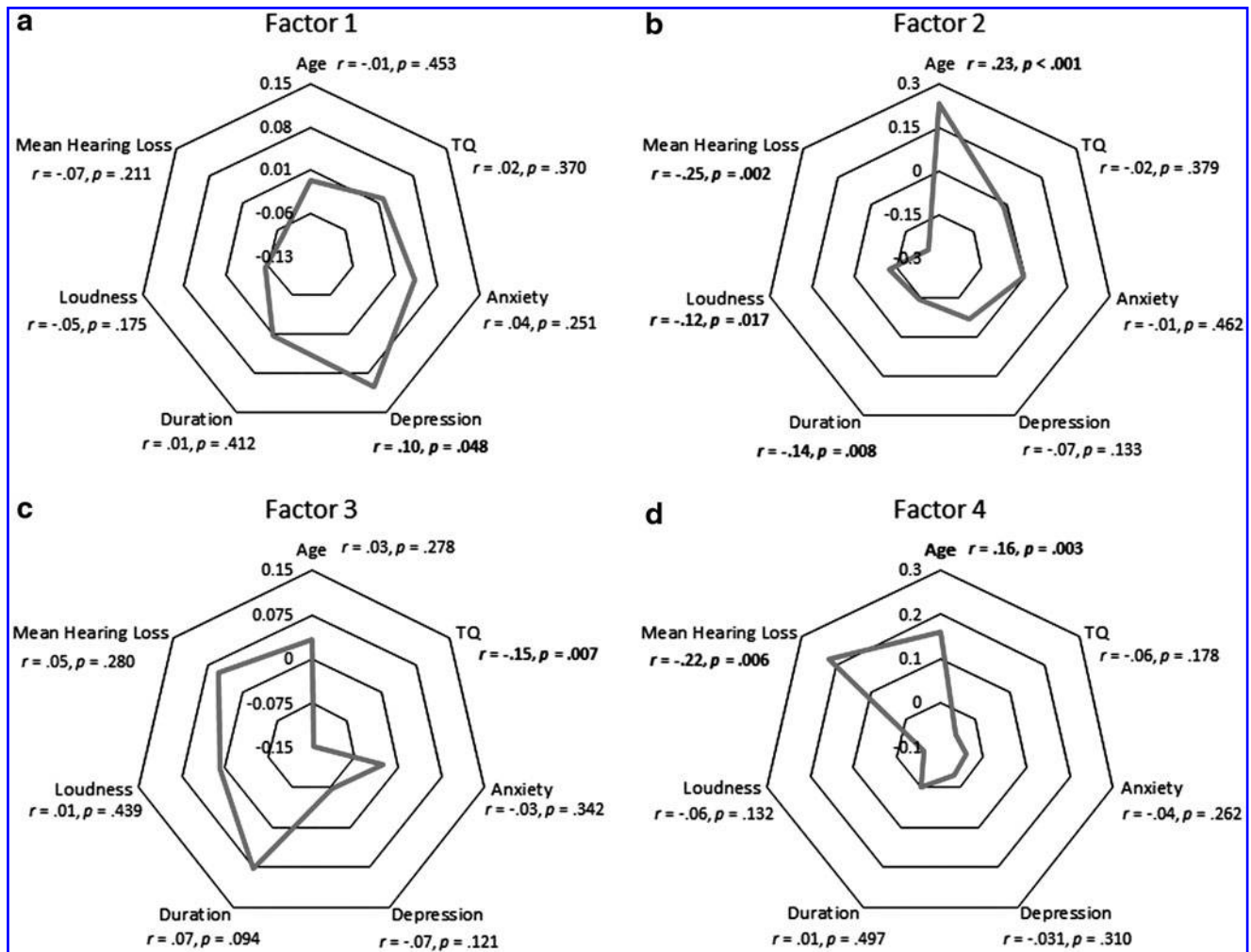


FIG. 5. Correlation of the factors and behavioral correlates. Correlations were deemed significant at $*p < 0.05$ and $**p < 0.01$ (one-tailed). (a) The correlation of Factor 1, (b) the correlation of Factor 2, (c) the correlation of Factor 3, and (d) the correlation of Factor 4 with the different behavioral measures.

MAE=0.38, and RMSE=0.50. The exclusivity of the prediction model was also significantly better at predicting tinnitus versus neuropathic pain patients compared to the averaged randomized prediction model ($\chi^2=21.31, p < 0.001$) (Fig. 2).

Discussion

With advancement in network theory, there is an increased interest to identify the neural signatures for the behavioral correlates of multisymptom disorders that could explain both, the mechanism of the underlying pathology as well as serve as a clinical diagnostic tool. This study aims at providing empirical evidence for behaviorally segregated, yet spatially and temporally overlapping functional modules that integrate in a disorder-specific way, resulting in a holistic experience that is unique to each pathology. In particular, we aim at establishing empirical evidence to the theoretical model for tinnitus, proposed by De Ridder and colleagues (2014b) and in doing so, present a possible clinical diagnostic tool for tinnitus.

The success of the model spun out using the k-fold cross-validation algorithm, in reliably discriminating cases with

tinnitus from controls significantly above chance is promising, especially considering the stringency and diminished bias of cross-validation testing (Lemm et al., 2011). Moreover, the statistical validity of the model is preserved when comparing the percentage of correctly and incorrectly classified cases with that of a random model. These results are in congruence with findings from other pathologies identified with functional network reorganization, including hepatic encephalopathy (Jao et al., 2015), autism spectrum disorder (Nomi and Uddin, 2015), pain (Wager et al., 2013), and migraine (Chong et al., 2016). In addition to the enhanced precision, the model displays a high degree of specificity by using only 65 out of 27,888 connections across all brain areas and frequencies to discriminate tinnitus from the control dataset. It is, however, important to note that these 65 connections only discriminate the tinnitus network from the control and hence the rest of the 27,822 connections are still common to both the tinnitus and the control network, but have been shown to be organized differently (Mohan et al., 2016a,b,c).

In agreement with our hypothesis, we observe from the correlation and partial correlation results that these 66 connections fall into clinically relevant factors that encode

TABLE 3. PARTIAL CORRELATION BETWEEN FACTORS AND BEHAVIORAL MEASURES

Behavioral measure	Controlling	Partial correlation			
		Factor 1	Factor 2	Factor 3	Factor 4
Age	Anxiety	-0.03	-0.23***	0.06	0.17**
	Duration	-0.02	-0.20**	0.01	0.17**
	Loudness	-0.003	-0.19***	0.02	0.18**
	MHL	0.01	-0.15*	0.21**	-0.05
TQ	Anxiety	0.10*	0.01	-0.14*	-0.04
	Depression	0.05	0.08	-0.12*	-0.05
	Duration	0.00	0.00	-0.15**	-0.06
	Loudness	0.05	0.01	-0.16**	-0.03
	MHL	0.03	0.10	-0.10	-0.05
Anxiety	Age	0.04	-0.05	-0.02	-0.02
	TQ	-0.02	-0.01	0.06	-0.02
	Depression	-0.02	0.04	0.02	-0.04
	Loudness	0.05	-0.01	-0.03	-0.04
Depression	TQ	0.04	-0.11*	0.04	0.01
	Anxiety	0.10	-0.08	-0.07	-0.002
	Loudness	0.10*	-0.07	-0.09	-0.004
	MHL	0.06	-0.09	-0.08	-0.02
Duration	Age	0.02	-0.12	0.06	-0.05
	TQ	0.06	-0.13	0.05	-0.01
	Loudness	0.03	-0.13	0.07	-0.01
	MHL	0.14	-0.14	-0.06	-0.14
Loudness	Age	-0.06	-0.08	0.002	-0.09
	TQ	-0.06	-0.10*	0.07	-0.04
	Anxiety	0.05	-0.08	0.03	-0.08
	Depression	0.02	-0.06	0.06	-0.08
	Duration	-0.05	-0.09	-0.04	-0.10
	MHL	-0.01	-0.01	0.05	-0.18*
MHL	Age	-0.06	-0.11	-0.10	0.20*
	TQ	-0.08	-0.27**	0.09	0.23**
	Depression	-0.07	-0.22**	0.08	0.23**
	Duration	-0.07	-0.20*	0.05	0.19*
	Loudness	-0.07	-0.23**	0.02	0.27**

* $p < 0.05$, ** $p < 0.01$, *** $p < 0.001$.

MHL, mean hearing loss; TQ, Tinnitus Questionnaire.

three important aspects of tinnitus—the sensory deprivation/memory of the deafferented frequency, tinnitus-related depression, and the salience associated with the tinnitus. We also observe that these connections cluster with respect to frequency bands in factors 2 (i.e., alpha2), 3 (i.e., delta), and 4 (i.e., alpha1), while factor 1 is mainly a combination of high frequencies (i.e., beta2 and gamma). Factors 2 and 4 seem to encode the aging and the hearing loss aspects of tinnitus, respectively. Although the model fairly discriminates between aging and hearing loss, auditory deprivation is one of the major effects of aging (Zagólski, 2006) and hence is difficult to tease apart the effect of one from the other (Francis et al., 2003; Huang and Tang, 2010). The tinnitus-related depression is encoded by factor 1, which in congruence with previous literature (De Ridder et al., 2011b; Husain and Schmidt, 2014; Schlee et al., 2009; Ueyama et al., 2013; Vanneste and De Ridder, 2011; Vanneste et al., 2010; Weisz et al., 2005) is encoded by the beta frequency bands. Other aspects of the emotional component of tinnitus are captured by the TQ (Adamchic et al., 2012; Belli et al., 2007; Crönlein et al., 2007; Kam et al., 2009; Meeus et al., 2007; Zeman et al., 2012), which corre-

lates with factor 3. Most of these connections fall in the delta band, which is associated with aiding long-distance connectivity and broadcasting information to other parts of the brain (Uhlhaas, 2013; von Stein and Sarnthein, 2000).

Physiologically, we observe that factors 2 and 4 consist of some of the important connections between the auditory cortex, parahippocampus, hippocampus, and orbitofrontal cortex, mostly communicating the Alpha2 frequency band. As mentioned above, these factors seem to be encoding ageing and hearing, respectively. The auditory deafferentation has been proposed to cause an increase in the oscillatory activity in the parahippocampus, which results in a lack of suppression of unimportant sensory information in the hippocampus (De Ridder and Vanneste, 2014). Furthermore, the factors also consist of areas that encode the pitch of the perceived tinnitus (De Ridder et al., 2014b), which has been shown to match the edge frequency of hearing loss (Moore, 2010; Sereda et al., 2015). In factor 1, most of the areas involved, such as the dorsal lateral prefrontal cortex, the connection between the rostral and bilateral pregenual anterior cingulate cortex, and the insula, form a part of the proposed distress network (De Ridder et al., 2014b; Schlee et al., 2009;

Ueyama et al., 2013) mostly found in the beta bands. Consistently, factor 1 also correlated with the tinnitus-related depression. Constant salience of the deprived sensory input in tinnitus (De Ridder and Vanneste, 2014; Sedley et al., 2015) triggers the salience network resulting in “aversive auditory pain” (De Ridder et al., 2011a). Some of the areas identified in factor 3 form a part of this salience network (Menon, 2015; Schlee et al., 2009; Seeley et al., 2007; Song et al., 2015). Since these connections are encoded in the delta band, we can expect that the salience and the “aversive pain” encoded in this factor are broadcasted throughout the brain. Furthermore, our tinnitus model presents evidence of statistical validity well above chance level even when tested against physiologically similar pathologies, such as neuropathic pain (De Ridder et al., 2011a, 2014a; Folmer et al., 2001; Isaacson et al., 2003; Møller, 1997). This unique property of our model not only shows that functional connectivity serves a better predictor to discriminating similar pathologies compared to neural activity (Hu and Iannetti, 2016) but also strongly concludes that the reorganization of the tinnitus network is distinguishably disorder specific.

From the results of this study, we can conclude that the neural synchronization captured by the functional connectivity strength is evident in carrying specific information in specific oscillatory bands, indicative of the theory of “communication through coherence” (Fries, 2005, 2015). It is important to keep in mind that although the 66 connections are reported to fall into distinct factors, this decision is made depending on their weighted contribution to that particular factor, implying that their contribution to the other factors is only less weighted as opposed to completely absent. It is because of this weighted contribution that the groups of connections may be considered part of overlapping modules encoding specific behavioral symptoms. Furthermore, this overlap among factors is observed to be spatial (i.e., have common regions among different factors), temporal (i.e., the same two regions communicate in different frequency bands), or spatiotemporal (i.e., a combination of both spatial and temporal overlap). Overlapping community structure is shown to be an inherent property of complex networks (Gregory, 2007; Palla et al., 2005; Shen et al., 2009; Yang and Leskovec, 2014) since it facilitates processing of multimodal input at specific nodes in the network (Wu et al., 2011). This increases the cost-efficiency of information processing since the same node takes part in multiple processing units. Overlapping communities are then integrated by a small number of long-distance connections (Bassett and Bullmore, 2006; Sporns and Zwi, 2004; Watts and Strogatz, 1998) that broadcast the unified information throughout the network, contributing to the cost-efficiency of information transfer (Bullmore and Sporns, 2012; Latora and Marchiori, 2003). In young healthy brain networks, cognitive processes such as attention, memory, and language are proposed to be handled by cognitively segregated yet functionally overlapping modules (Mesulam, 1990). In the case of a neuropathology, we observe that the functional network undergoes a disorder-specific spatiotemporal overlap of groups of connections that are responsible for segregated encoding of the behavioral symptoms exclusive to the disorder. Such reorganization promotes an undesirable efficiency in the wiring of the disease network (Mohan et al.,

2016c) and broadcasting of pathological symptoms throughout the brain.

The presence of functionally overlapping modules in the brain presents an efficient way of sending information through the physical anatomical connection between different regions. The concept of different frequency bands carrying unique packets of information through the same physical channel is termed multiplexing (Panzeri et al., 2010). Multiplexing allows selective processing of information and switching between different functional networks (Akam and Kullmann, 2014). This method allows different brain areas to engage in different networks (Akam and Kullmann, 2014) and can hence allow efficient processing of multimodal input at the same location. Although, sometimes, there may be only one physical connection between two brain areas, multiplexing allows different types of information to be transmitted to-and-fro the same line (Weinstein and Ebert, 1971). In this study, we not only observe the presence of spatial, temporal, and spatiotemporally overlapping functional networks but also a unique frequency-specific encoding of behavioral information. This alludes to the possibility of information being communicated between different regions by means of multiplexing. Multiplexing together with spatiotemporal overlap of functional modules may not only improve the efficiency of information transfer but also gives the brain more degrees of freedom to compensate for the disorder. The application of the concept of multiplexing to the brain is relatively new and hence opens avenues of investigation of efficient transmission of information between different brain regions.

Although this study provides a wealth of information about tinnitus organization, there are some limitations to the study that have to be addressed. Although the tinnitus and control groups have comparable average age ranges, they are not controlled for hearing loss. To avoid issues of statistical power in machine learning algorithms and to look at the general effects of tinnitus versus no tinnitus, a control for hearing loss was not applied. This study, however, paves way for future studies to look into groups that have a more stringent control on the inclusion criteria of the study. Second, although EEG source localization is gaining traction, it is still a statistical approximation of the sources of cortically generated potentials. Also, the method cannot reliably identify subcortical structures such as the thalamus, nucleus accumbens, amygdala, and parts of the basal ganglia that have also been shown to play an important role in tinnitus (Llinás et al., 2005; Maudoux et al., 2012; Rauschecker et al., 2010). It would be worthwhile to replicate this study using functional magnetic resonance imaging (fMRI) to confirm and add valuable information to the findings of this study. Despite these limitations, this study has the advantage of temporal resolution to look into the connections between different regions on different scales of cortical oscillations. Moreover, different connectome studies are allowing significant improvement in target selection for invasive and noninvasive brain stimulation therapies (Crossley et al., 2014), and our findings may allow an even more specific selection of target that can be tailored to the therapeutic needs of individual patients. Due to the integration of multimodal subnetworks, there has recently been a push for classifying patients on a symptom spectrum rather than the more standard categorical diagnoses to account for individual patient

differences across a group of symptoms (Buckholtz and Meyer-Lindenberg, 2012). Coupled with recent investigations in connectome changes across the lifespan that could serve as a baseline (Cao et al., 2014), identification of separable subnetworks, along with their behavioral correlates and the quantification of alterations in connectivity strength from resting-state data, could become one of the most powerful and individualized biomarkers of neurological pathologies (Kaiser, 2013).

Conclusion

Our study shows a disorder-specific reorganization in the tinnitus network as behaviorally segregated, spatiotemporally overlapping subnetworks providing empirical evidence to the theoretical tinnitus model proposed by De Ridder and colleagues. The frequency-specific encoding of behavioral symptoms between overlapping functional modules suggests the presence of multiplexing in the brain, which allows for different types of information to be transmitted through the same anatomical connection. This type of reorganization can also be viewed as a compensation mechanism of the brain to multisymptom disorders presenting an undesired efficiency of the disease network. Specific to tinnitus, the exclusivity of the model and behavioral categorization of connections could potentially become a clinical tool that might objectively diagnose the disorder.

Author Disclosure Statement

No competing financial interests exist.

References

- Adamchic I, Tass PA, Langguth B, Hauptmann C, Koller M, Schecklmann M, et al. 2012. Linking the Tinnitus Questionnaire and the subjective Clinical Global Impression: which differences are clinically important? *Health Qual Life Outcomes* 10:79.
- Agosta F, Sala S, Valsasina P, Meani A, Canu E, Magnani G, Cappa SF, et al. 2013. Brain network connectivity assessed using graph theory in frontotemporal dementia. *Neurology* 81:134–143.
- Akam T, Kullmann DM. 2014. Oscillatory multiplexing of population codes for selective communication in the mammalian brain. *Nat Rev Neurosci* 15:111–122.
- Albert R, Albert I, Nakarado GL. 2004. Structural vulnerability of the North American power grid. *Phys Rev E* 69:025103.
- Axelsson A, Ringdahl A. 1989. Tinnitus—a study of its prevalence and characteristics. *Br J Audiol* 23:53–62.
- Barabasi A-L, Gulbahce N, Loscalzo J. 2011. Network medicine: a network-based approach to human disease. *Nat Rev Genet* 12:56–68.
- Bassett DS, Bullmore E. 2006. Small-world brain networks. *Neuroscientist* 12:512–523.
- Bassett DS, Bullmore E, Verchinski BA, Mattay VS, Weinberger DR, Meyer-Lindenberg A. 2008. Hierarchical organization of human cortical networks in health and schizophrenia. *J Neurosci* 28:9239–9248.
- Belli S, Belli H, Bahcebası T, Ozcetin A, Alpay E, Ertem U. 2007. Assessment of psychopathological aspects and psychiatric comorbidities in patients affected by tinnitus. *Eur Arch Otorhinolaryngol* 265:279–285.
- Buckholtz JW, Meyer-Lindenberg A. 2012. Psychopathology and the human connectome: toward a transdiagnostic model of risk for mental illness. *Neuron* 74:990–1004.
- Bullmore E, Sporns O. 2009. Complex brain networks: graph theoretical analysis of structural and functional systems. *Nat Rev Neurosci* 10:186–198.
- Bullmore E, Sporns O. 2012. The economy of brain network organization. *Nat Rev Neurosci* 13:336–349.
- Cao M, Wang JH, Dai ZJ, Cao XY, Jiang LL, Fan FM, et al. 2014. Topological organization of the human brain functional connectome across the lifespan. *Dev Cogn Neurosci* 7:76–93.
- Chong CD, Gaw N, Fu Y, Li J, Wu T, Schwedt TJ. 2016. Migraine classification using magnetic resonance imaging resting-state functional connectivity data. *Cephalalgia*, 0333102416652091.
- Cohen R, Erez K, ben-Avraham D, Havlin S. 2000. Resilience of the Internet to random breakdowns. *Phys Rev Lett* 85:4626–4628.
- Cohen R, Erez K, ben-Avraham D, Havlin S. 2001. Breakdown of the Internet under intentional attack. *Phys Rev Lett* 86:3682–3685.
- Congedo M. 2002. *EureKa!* (Version 3.0) [Computer Software]. Knoxville, TN: NovaTech EEG Inc. Available: www.NovaTechEEG.
- Congedo M, John RE, De Ridder D, Prichep L, Isenhardt R. 2010. On the “dependence” of “independent” group EEG sources; an EEG study on two large databases. *Brain Topogr* 23:134–138.
- Crönlein T, Langguth B, Geisler P, Hajak G. 2007. Tinnitus and insomnia. *Prog Brain Res* 166:227–233.
- Crossley NA, Mechelli A, Scott J, Carletti F, Fox PT, McGuire P, Bullmore ET. 2014. The hubs of the human connectome are generally implicated in the anatomy of brain disorders. *Brain* 137:2382–2395.
- De Ridder D, Congedo M, Vanneste S. 2015. The neural correlates of subjectively perceived and passively matched loudness perception in auditory phantom perception. *Brain Behav* 5:e00331.
- De Ridder D, Elgoyhen AB, Romo R, Langguth B. 2011a. Phantom percepts: tinnitus and pain as persisting aversive memory networks. *Proc Natl Acad Sci* 108:8075–8080.
- De Ridder D, Song J-J, Vanneste S. 2013. Frontal cortex TMS for tinnitus. *Brain Stimul* 6:355–362.
- De Ridder D, Vanneste S. 2014. Targeting the parahippocampal area by auditory cortex stimulation in tinnitus. *Brain Stimul* 7:709–717.
- De Ridder D, Vanneste S, Congedo M. 2011b. The distressed brain: a group blind source separation analysis on tinnitus. *PLoS One* 6:e24273.
- De Ridder D, Vanneste S, Freeman W. 2014a. The Bayesian brain: phantom percepts resolve sensory uncertainty. *Neurosci Biobehav Rev* 44:4–15.
- De Ridder D, Vanneste S, Weisz N, Londero A, Schlee W, Elgoyhen AB, Langguth B. 2014b. An integrative model of auditory phantom perception: tinnitus as a unified percept of interacting separable subnetworks. *Neurosci Biobehav Rev* 44:16–32.
- Eskildsen SF, Coupé P, Fonov VS, Pruessner JC, Collins DL. 2015. Structural imaging biomarkers of Alzheimer’s disease: predicting disease progression. *Neurobiol Aging* 36 Suppl 1: S23–S31.
- Folmer RL, Griest SE, Martin WH. 2001. Chronic tinnitus as phantom auditory pain. *Otolaryngol Head Neck Surg* 124:394–400.

- Fornito A, Zalesky A, Breakspear M. 2015. The connectomics of brain disorders. *Nat Rev Neurosci* 16:159–172.
- Francis HW, Ryugo DK, Gorelikow MJ, Prosen CA, May BJ. 2003. The functional age of hearing loss in a mouse model of presbycusis. II. Neuroanatomical correlates. *Hear Res* 183:29–36.
- Fries P. 2005. A mechanism for cognitive dynamics: neuronal communication through neuronal coherence. *Trends Cogn Sci* 9:474–480.
- Fries P. 2015. Rhythms for cognition: communication through coherence. *Neuron* 88:220–235.
- Goh K-I, Cusick ME, Valle D, Childs B, Vidal M, Barabási A-L. 2007. The human disease network. *Proc Natl Acad Sci* 104:8685–8690.
- Gregory S. 2007. An algorithm to find overlapping community structure in networks. In: Kok JN, Koronacki J, Lopez de Mantaras R, Matwin S, Mladenić D, Skowron A (eds.) *Knowledge Discovery in Databases: PKDD 2007: 11th European Conference on Principles and Practice of Knowledge Discovery in Databases*. Warsaw, Poland, September 17–21, 2007. Proceedings. Springer Berlin Heidelberg, Berlin, Heidelberg; pp. 91–102.
- Hu L, Iannetti GD. 2016. Painful issues in pain prediction. *Trends Neurosci* 39:212–220.
- Huang Q, Tang J. 2010. Age-related hearing loss or presbycusis. *Eur Arch Otorhinolaryngol* 267:1179–1191.
- Husain FT, Schmidt SA. 2014. Using resting state functional connectivity to unravel networks of tinnitus. *Hear Res* 307:153–162.
- Isaacson JE, Moyer MT, Schuler HG, Blackall GF. 2003. Clinical associations between tinnitus and chronic pain. *Otolaryngol Head Neck Surg* 128:706–710.
- Jao T, Schroter M, Chen CL, Cheng YF, Lo CY, Chou KH, et al. 2015. Functional brain network changes associated with clinical and biochemical measures of the severity of hepatic encephalopathy. *Neuroimage* 122:332–344.
- Jastreboff PJ. 1990. Phantom auditory perception (tinnitus): mechanisms of generation and perception. *Neurosci Res* 8:221–254.
- Kaiser M. 2013. The potential of the human connectome as a biomarker of brain disease. *Front Hum Neurosci* 7:484.
- Kam ACS, Cheung APP, Chan PYB, Leung EKS, Wong TKC, Tong MCF, van Hasselt A. 2009. Psychometric properties of a Chinese (Cantonese) version of the Tinnitus Questionnaire. *Int J Audiol* 48:568–575.
- Lancaster JL, Woldorff MG, Parsons L, Liotti M, Freitas C, Rainey L, et al. 2000. Automated Talairach atlas labels for functional brain mapping. *Hum Brain Mapp* 10:120–131.
- Latora V, Marchiori M. 2003. Economic small-world behavior in weighted networks. *Eur Phys J B* 32:249–263.
- Lemm S, Blankertz B, Dickhaus T, Müller K-R. 2011a. Introduction to machine learning for brain imaging. *NeuroImage* 56:387–399.
- Llinás R, Urbano FJ, Leznik E, Ramírez RR, van Marle HJF. 2005. Rhythmic and dysrhythmic thalamocortical dynamics: GABA systems and the edge effect. *Trends Neurosci* 28:325–333.
- Maudoux A, Lefebvre P, Cabay J-E, Demertzi A, Vanhauzenhuyse A, Laureys S, Soddu A. 2012. Auditory resting-state network connectivity in tinnitus: a functional MRI Study. *PLoS One* 7:e36222.
- Meeus O, Blaivie C, Van de Heyning P. 2007. Validation of the Dutch and the French version of the Tinnitus Questionnaire. *B-ENT* 3 Suppl 7:11–17.
- Meeus O, De Ridder D, Van de Heyning P. 2011. Administration of the combination clonazepam-deanxit as treatment for tinnitus. *Otol Neurotol* 32:701–709.
- Meeus O, Heyndrickx K, Lambrechts P, De Ridder D, Van de Heyning P. 2010. Phase-shift treatment for tinnitus of cochlear origin. *Eur Arch Otorhinolaryngol* 267:881–888.
- Menon V. 2015. *Salience Network A2-Toga, Arthur W. Brain Mapping*. Waltham: Academic Press. pp. 597–611.
- Mesulam M. 1990. Large-scale neurocognitive networks and distributed processing for attention, language, and memory. *Ann Neurol* 28:597–613.
- Meunier D, Achard S, Morcom A, Bullmore E. 2009. Age-related changes in modular organization of human brain functional networks. *NeuroImage* 44:715–723.
- Meunier D, Lambiotte R, Bullmore ET. 2010. Modular and hierarchically modular organization of brain networks. *Front Neurosci* 4:200.
- Mohan A, De Ridder D, Vanneste S. 2016a. Emerging hubs in phantom perception connectomics. *Neuroimage Clin* 11:181–194.
- Mohan A, De Ridder D, Vanneste S. 2016b. Graph theoretical analysis of brain connectivity in phantom sound perception. *Scientific Rep* 6:19683.
- Mohan A, De Ridder D, Vanneste S. 2016c. Robustness and dynamicity of functional networks in phantom sound. *Neuroimage* 146:171–187.
- Møller AR. 1997. Similarities between chronic pain and tinnitus. *Otol Neurotol* 18:577–585.
- Moore BC. 2010. The relationship between tinnitus pitch and the edge frequency of the audiogram in individuals with hearing impairment and tonal tinnitus. *Hear res* 261:51–56.
- Nomi JS, Uddin LQ. 2015. Developmental changes in large-scale network connectivity in autism. *Neuroimage Clin* 7:732–741.
- Olde Dubbelink KTE, Hillebrand A, Stoffers D, Deijen JB, Twisk JWR, Stam CJ, Berendse HW. 2014. Disrupted brain network topology in Parkinson's disease: a longitudinal magnetoencephalography study. *Brain* 137:197–207.
- Palla G, Derenyi I, Farkas I, Vicsek T. 2005. Uncovering the overlapping community structure of complex networks in nature and society. *Nature* 435:814–818.
- Panzeri S, Brunel N, Logothetis NK, Kayser C. 2010. Sensory neural codes using multiplexed temporal scales. *Trends Neurosci* 33:111–120.
- Papo D, Buldu JM, Boccaletti S, Bullmore ET. 2014. Complex network theory and the brain. *Philos Trans R Soc Lond B Biol Sci* 369:20130520.
- Pascual-Marqui RD. 2002. Standardized low-resolution brain electromagnetic tomography (sLORETA): technical details. *Methods Find Exp Clin Pharmacol* 24:5–12.
- Pascual-Marqui RD, Lehmann D, Koukkou M, Kochi K, Anderer P, Saletu B, et al. 2011. Assessing interactions in the brain with exact low-resolution electromagnetic tomography. *Philos Trans A Math Phys Eng Sci* 369:3768–3784.
- Plitt M, Barnes KA, Wallace GL, Kenworthy L, Martin A. 2015. Resting-state functional connectivity predicts longitudinal change in autistic traits and adaptive functioning in autism. *Proc Natl Acad Sci* 112:E6699–E6706.
- Rauschecker JP, Leaver AM, Muhlau M. 2010. Tuning out the noise: limbic-auditory interactions in tinnitus. *Neuron* 66:819–826.
- Roelofs J, Peters ML, McCracken L, Vlaeyen JW. 2003. The pain vigilance and awareness questionnaire (PVAQ): further psychometric evaluation in fibromyalgia and other chronic pain syndromes. *Pain* 101:299–306.
- Schlee W, Mueller N, Hartmann T, Keil J, Lorenz I, Weisz N. 2009. Mapping cortical hubs in tinnitus. *BMC Biol* 7:80–80.

- Sedley W, Gander PE, Kumar S, Oya H, Kovach, Christopher K, Nourski, Kirill V, et al. 2015. Intracranial mapping of a cortical tinnitus system using residual inhibition. *Curr Biol* 25:1208–1214.
- Seeley WW, Menon V, Schatzberg AF, Keller J, Glover GH, Kenna H, et al. 2007. Dissociable intrinsic connectivity networks for salience processing and executive control. *J Neurosci* 27:2349–2356.
- Sereda M, Edmondson-Jones M, Hall DA. 2015. Relationship between tinnitus pitch and edge of hearing loss in individuals with a narrow tinnitus bandwidth. *Int J Audiol* 54:249–256.
- Shargorodsky J, Curhan GC, Farwell WR. 2010. Prevalence and characteristics of tinnitus among US adults. *Am J Med* 123:711–718.
- Shen H, Cheng X, Cai K, Hu M-B. 2009. Detect overlapping and hierarchical community structure in networks. *Physica A* 388:1706–1712.
- Skidmore F, Korenkevych D, Liu Y, He G, Bullmore E, Pardalos PM. 2011. Connectivity brain networks based on wavelet correlation analysis in Parkinson fMRI data. *Neurosci Lett* 499:47–51.
- Song JJ, Vanneste S, Lazard DS, Van de Heyning P, Park JH, Oh SH, De Ridder D. 2015. The role of the salience network in processing lexical and nonlexical stimuli in cochlear implant users: an ALE meta-analysis of PET studies. *Hum Brain Mapp* 36:1982–1994.
- Sporns O, Zwi JD. 2004. The small world of the cerebral cortex. *Neuroinformatics* 2:145–162.
- Stam CJ, de Haan W, Daffertshofer A, Jones BF, Manshanden I, van Cappellen van Walsum, et al. 2009. Graph theoretical analysis of magnetoencephalographic functional connectivity in Alzheimer's disease. *Brain* 132:213–224.
- Strogatz SH. 2001. Exploring complex networks. *Nature* 410:268–276.
- Tonndorf J. 1987. The analogy between tinnitus and pain: a suggestion for a physiological basis of chronic tinnitus. *Hear Res* 28:271–275.
- Ueyama T, Donishi T, Ukai S, Ikeda Y, Hotomi M, Yamanaka N, et al. 2013. Brain regions responsible for tinnitus distress and loudness: a resting-state fMRI Study. *PLoS One* 8:e67778.
- Uhlhaas PJ. 2013. Dysconnectivity, large-scale networks and neuronal dynamics in schizophrenia. *Curr Opin Neurobiol* 23:283–290.
- Vanneste S, De Ridder D. 2011. Bifrontal transcranial direct current stimulation modulates tinnitus intensity and tinnitus-distress-related brain activity. *Eur J Neurosci* 34:605–614.
- Vanneste S, Plazier M, der Loo Ev, de Heyning PV, Congedo M, De Ridder D. 2010. The neural correlates of tinnitus-related distress. *Neuroimage* 52:470–480.
- von Stein A, Sarnthein J. 2000. Different frequencies for different scales of cortical integration: from local gamma to long range alpha/theta synchronization. *Int J Psychophysiol* 38:301–313.
- Wager TD, Atlas LY, Lindquist MA, Roy M, Woo C-W, Kross E. 2013. An fMRI-based neurologic signature of physical pain. *N Engl J Med* 368:1388–1397.
- Watts DJ, Strogatz SH. 1998. Collective dynamics of 'small-world' networks. *Nature* 393:440–442.
- Weinstein S, Ebert P. 1971. Data transmission by frequency-division multiplexing using the discrete fourier transform. *IEEE Trans Commun Technol* 19:628–634.
- Weisz N, Moratti S, Meinzer M, Dohrmann K, Elbert T. 2005. Tinnitus perception and distress is related to abnormal spontaneous brain activity as measured by magnetoencephalography. *PLoS Med* 2:e153.
- Wu K, Taki Y, Sato K, Sassa Y, Inoue K, Goto R, et al. 2011. The overlapping community structure of structural brain network in young healthy individuals. *PLoS One* 6:e19608.
- Yang J, Leskovec J. 2014. Overlapping communities explain core-periphery organization of networks. *Proc IEEE Annu Northeast Bioeng Conf* 102:1892–1902.
- Zagólski O. 2006. Management of tinnitus in patients with presbycusis. *Int Tinnitus J* 12:175.
- Zeman F, Koller M, Schecklmann M, Langguth B, Landgrebe M. 2012. Tinnitus assessment by means of standardized self-report questionnaires: Psychometric properties of the Tinnitus Questionnaire (TQ), the Tinnitus Handicap Inventory (THI), and their short versions in an international and multi-lingual sample. *Health Qual Life Outcomes* 10:1–10.

Address correspondence to:

*Sven Vanneste
Laboratory for Clinical and Integrative Neuroscience
School of Behavioral and Brain Sciences
University of Texas at Dallas
800W Campbell Road
Richardson, TX 75080*

E-mail: sven.vanneste@utdallas.edu